Shaping Copper Nanocatalysts to Steer Selectivity in the CO₂ Electrochemical Reduction Reaction

Kevin Rossi [1], Raffaella Buonsanti, [1]*

[1] Laboratory of Nanochemistry for Energy (LNCE), Department of Chemical Sciences and Engineering, École Polytechnique Fédérale de Lausanne, CH-1950 Sion, Switzerland.

* raffaella.buonsanti@epfl.ch

Conspectus

The carbon-neutral production of fuels and chemical feedstocks is one of the grand-challenges for our society to solve. The electrochemical conversion of CO_2 is emerging as a promising technology contributing towards this goal. Despite the huge progress made over the last decade, selectivity still remains a challenge. This Account presents an overview of recent advancements in the design of selective catalysts by exploiting the structural sensitivity of the CO_2 electrochemical reduction reaction (CO_2RR). In particular, it shows that the accurate and precise control of the shape and size of Cu nanocatalysts is instrumental in understanding and in discovering the structure-selectivity relationships governing the reduction of CO_2 towards valuable hydrocarbons, such as methane and ethylene. It further illustrates the use of faceted Cu nanocatalysts to interrogate catalytic pathways and to increase selectivity towards oxygenates, such as ethanol, in the framework of tandem schemes. The last part of the Account addresses reconstructions of these well-defined catalysts, in ways which can both degrade or improve the catalyst performance, and stresses the importance of identifying the reconstruction mechanisms. Finally, an outlook on the emerging paradigms which will empower the design of novel catalysts for CO_2RR concludes the Account.

Key References:

Loiudice A., Lobaccaro P., Kamali E. A., Thao T., Huang B. H., Ager J. W., Buonsanti R.. Tailoring copper nanocrystals towards C_2 products in electrochemical CO_2 reduction. Angewandte Chemie International Edition **2016**, 55 (19), 5789-5792.[1] *Here, we reveal a non-monotonic size-dependence in the selectivity of copper nanocrystals with a cubic shape for CO$_2$RR. We synthesize size-selected and shape-controlled cubes with edge length equal to 24nm, 44nm, and 63nm by colloidal chemistry methods. We find that the 44nm Cu nano-cubes exhibit the highest selectivity towards CO$_2$RR and faradaic efficiency for ethylene.*

Iyengar P., Huang J., De Gregorio G.L., Gadiyar C., Buonsanti R. Size dependent selectivity of Cu nano-octahedra catalysts for the electrochemical reduction of CO_2 to CH_4. Chemical Communications **2020**, 55 (60), 8796-8799.[2] *Here, we establish the size-dependent selectivity and faradaic efficiency trends for CO2RR of copper nanocrystals with an octahedral shape. We exploit free variables in colloidal chemistry to control the catalyst size and look at three of them, namely 75, 110 and 310 nm. We observe that the smallest among the three, the 75 nm sample, displays the highest CO$_2$RR selectivity and faradaic efficiency for CO$_2$ conversion into methane.*

Iyengar P., Kolb M.J., Pankhurst J.R., Calle-Vallejo F., Buonsanti R. Elucidating the Facet-Dependent Selectivity for CO_2 Electroreduction to Ethanol of Cu–Ag Tandem Catalysts. ACS Catalysis **2021**, 11 (8), 4456-4463.[3] *Here we exploit tandem catalysis and shape-controlled cubic and octahedral Cu nanocrystals to selectively obtain ethanol as the majority product in CO$_2$RR. By comparing the faradaic efficiencies and partial current densities observed in the Cu catalysts with the two different shapes, we isolate the favoured pathway which leads to ethanol production, the *CH$_x$–*CO coupling, and identify the octahedral copper as the most selective towards this alcohol.*

Vavra J., Shen T., Stoian D., Tileli V., Buonsanti R. Real-time Monitoring Reveals Dissolution/Redeposition Mechanism in Copper Nanocatalysts during the Initial Stages of the CO_2 Reduction Reaction, Angewandte Chemie International Edition **2021**, 60 (3), 1347-1354.[4] *Here we shed light on the mechanism through which Cu nanosphere modify their size and*

morphology during the CO₂RR start-up phase. In situ TEM and operando XAS inform us that the restructuring of the catalysts involves the dissolution and redeposition of Cu transient species in solution.

1. INTRODUCTION

The electrochemical CO_2 reduction reaction (CO₂RR) into energy carriers and chemical feedstocks is an attractive solution to curb atmospheric CO_2 levels, close the carbon-loop in the making of value-added chemicals, and provide long-term storage for excess energy from renewable sources.[5,6] A few pilot scale industrial projects have been launched in the last few years. Among the most notables, Evonik and Siemens Energy are currently testing the use of metallic catalyst to convert CO_2 captured from the atmosphere into CO, the latter than being fed to bacteria which convert it into multi-carbon products such as hexanol and buthanol.[7] AirCO started to commercialize products leveraging high purity alcohols obtained from CO₂RR.[8] Twelve owns a patent about a modular and scalable electrochemical reactor to synthesize carbon-based feedstocks from CO_2.[9] Despite this huge progress in the last decade, one of the current challenges in CO₂RR is to find catalysts which render this conversion selective towards one specific product.

As of today, Cu still remains the only single metal catalyst ones able to generate high energy dense hydrocarbons and alcohols, going beyond the simple CO molecule, with reasonable efficiencies.[10] Beside empirical evidence originating from experiments, DFT calculations help to rationalize the unique property of Cu based catalysts based on the interactions of CO and hydrogen with the surface of late transition metals.[11,12] While the CO weakly binding Ag and Au convert CO_2 to CO, the Cu intermediate binding energy towards CO is ideal to favor its conversion into more valuable C_1 and C_2 products.[11,12] While unique in its behavior, polycrystalline copper foil produces more than 16 different products, which is extremely inconvenient for industrial implementation.[13]

Experiments conducted on single crystals have played a prominent role in deciphering the structure - property relationships which determine the Cu catalyst selectivity towards one product or another.[14-17] The milestone work by Hori comprised the systematic assessment of the performance of 19 single crystal Cu surfaces at different applied potential.[14] A few years ago Hahn et al. [15] and

Huang et al. [16] further provided a systematic report on the potential-dependent behavior of Cu (111), (100), (110) and (751) surfaces. Structure-dependent selectivity trends emerged clearly from these three studies. The (100) and (111) surfaces promote ethylene and methane formation, respectively. Stepped and high Miller index facets - e.g., (751) and (551) - are selective for multicarbon products and oxygenates. Schouten et al. [17] investigated CO_2RR on (322) (5(111)x(100) orientation) and (911) (5(100)x(111) orientation) surfaces to discriminate whether (100) steps or terraces were active and selective towards ethylene production. The latter was significant only on (911) surfaces at low overpotential, which reinforced the importance of (100) terraces in this CO_2 reduction pathway.

While studies on single crystals are instrumental towards a fundamental understanding of the chemistry involved, they are often performed in conditions and with catalysts which are too far from those under which an industrial electrochemical reactor would operate. Experiments aimed at addressing this gap between the conditions of model experiments and the realistic operating conditions are therefore needed. [18,19]

In this Account, we discuss recent advancements in the use of shape-controlled Cu nanocatalysts to uncover the design rules for selective catalysts in CO_2RR. We will argue that well-defined nanocrystals (NCs), with monodispersed size and homogeneous morphologies, serve the purpose of testing and translating the discoveries from single crystal studies and the predictions drawn from theoretical models as well as revealing new insight into catalytic pathways. By describing the most significant milestones reached by us and others, we will show how the exquisite control of Cu nanocatalyst size and shape enables to unveil non-trivial structure-property relationships and ultimately tune the CO_2RR selectivity towards methane, ethane, and ethanol. We will then detail the catalysts restructuring mechanisms, detailed by operando studies, and discuss examples about how these can be either detrimental or beneficial, depending on the initial shape of the catalysts. We will finally conclude the Account with an outlook on the emerging trends and open questions towards the design of selective CO_2RR catalysts.

2. SYNTHESIS OF SHAPE-CONTROLLED Cu NANOCATALYSTS

An exquisite control on the size and shape of nanocatalysts is a necessary step towards univocally establishing robust structure-property relationships.[20-26] The synthesis of samples which are monodisperse in size and display morphological homogeneity is a non-trivial task. Several synthetic methods are available and each of them possess pros and cons. Here, we comment on those which have been utilized so far for size- and/or shape- controlled Cu nanocatalysts.

The simplest method is the inverse micelle encapsulation. Here, non-polar/polar block copolymers, or other amphiphilic molecules, are dissolved in a non-polar solvent to form reverse micelles. The micelles are loaded with Cu precursors and stirred at a certain temperature to form Cu NCs. Generally, only spherical NCs are obtained but their size is easily tunable by varying the polymer nature, particularly the length of the carbon chain and the polarity of the polymer head. Reske et al utilized inverse micelle encapsulation to synthesize Cu spheres, with size between 2 and 15 nm.[27] A good control of the shape polydispersity was achieved, while the size distribution displayed a relatively standard deviation close to 30% of the mean value.

Electrochemical cycling represents another method to nanostructure and to tune the exposed facets of Cu electrodes. In a nutshell, cycling between the oxidizing and the reducing potential is utilized to restructure a metallic surface, often in the presence of ions in the electrolyte as structure directing agents. Generally, this method is suitable for nanocatalysts with size above 100nm and very fine tuning of the size is not possible. Cu cubes have been synthesized by potential cycling of Cu foil in the presence of potassium halides, where the number of cycles was utilized to tune their size. The seminal work by Roberts et al. [28] produced Cu cubes of around 100 nm while mesoscale cuboids of size 400-500nm were synthesized by Chen at al. [29] The same synthetic route was later adopted by Grosse et al. [30] to make samples with size equal to 222, 457, 1013 nm. In all these cases the size distribution found a ~20% standard deviation.

Among the others, colloidal chemistry emerges as the most versatile approach in terms of tunability of nanocatalysts with monodispersed sizes and homogeneous shapes.[23-26] Here,

precursor solutions are heated to form monomers, which then nucleate and generate nanocrystals. Colloidal synthesis enables an exquisite control over the size (with standard deviation < 10%) and shape of the NCs by manipulating the the reaction solvent, the reaction temperature and time, the precursor chemistry and concentration, the organic ligands which interact with the precursor as well as passivate the NC surface. Manthiram et al. [31] first reported on spherical NCs with size 7 nm, later our group developed protocols to synthesize cubes with defined sizes between 15 and 80 nm [1,32,33], octahedra with sizes between 75 and 310 nm [2,33], and tetrahedra [33], while Choi et al. [34] drew a route towards the making of Cu penta-fold twinned star decahedra. An overview of the size and shape-controlled Cu NCs synthesized by means of colloidal chemistry is reported in Figure 1. In addition to homogeneous nucleation from a precursor solution, colloidal synthesis offers the possibility to exploit seeded growth as an alternative approach to tune NC size and shape. Pre-formed NC seeds are utilized to direct monomers nucleation and eventually the growth of a second material. Pd seeds were utilized by Wang et al. to synthesise nanocubes with size ~40 nm first. [35] Then, they utilized Se as an etchant to expose (110) facets at the expense of (100) ones which lead to the formation of truncated nanocubes and rhombic dodecahedra.[35]
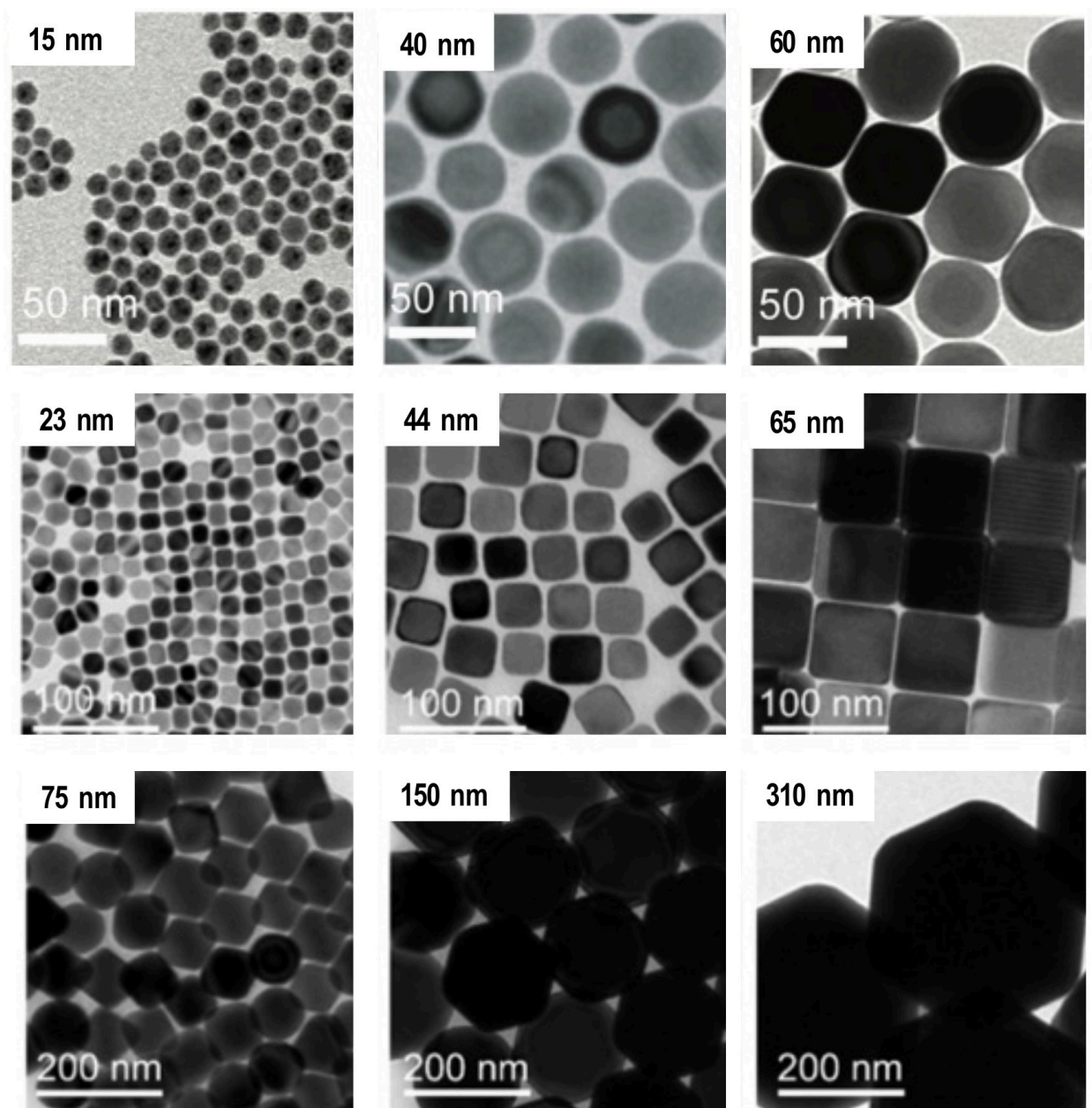
Figure 1. Representative transmission electron microscopy (TEM) images of Cu NCs with different shapes (spheres, cubes and octahedra) synthesized be means of colloidal chemistry. Adapted with permission from [32], Copyright Nature Springer and from [2], Copyright Royal Society of Chemistry.

3. IMPACT OF NANOCATALYSTS' SIZE AND SHAPE ON CO$_2$RR SELECTIVITY

In this section, we offer an overview of the size- and shape-dependent selectivity trends observed in Cu nanocatalysts. Spheres were the first well-defined NCs investigated in the literature. According to the Wulff construction, the most table shape for NCs of few to several nanometers is a truncated octahedron terminated by (111) and (100) facets, which appear as a « sphere » in electron microscopy images.[36] Reske et al. [27] performed a very systematic study of Cu spheres with size between 2 and 15 nm as CO$_2$RR electrocatalysts. The key finding of this study was that hydrocarbons production drops below 5 nm, with no ethylene and little methane being produced by spheres of diameter below 2nm. The authors put forward a site-counting model to rationalize the observed data, and suggested that low-coordination sites, abundant in small NCs, are not active towards hydrocarbon. Later on, our experiments on Cu spheres with size 7 and 27 nm confirmed that HER dominates over CO$_2$RR at -1.1 V$_{RHE}$ (RHE=Reversible Hydrogen Electrode). [1] In contrast, Manthiram et al. [31] found that 7 nm Cu spheres produce methane in the 1.05 - 1.15 V$_{RHE}$ range. Concomitantly, they reported on significant morphological changes during the course of CO$_2$RR, resulting in the formation of polycrystalline catalysts with size 14-32 nm. The authors concluded that Cu spheres display active sites for methane production which are then lost during reconstruction. Mistry et al. [37] et al later deconvoluted the effect of NC size and distance on CO$_2$RR selectivity and explained that the selectivity towards CO$_2$RR decreases as the interparticle distance decreases due to pH and mass transfer effects. More recently, Kim et al. [38] highlighted the importance of loading (i.e., interparticle distance) on reconstruction processes, with high loadings fostering the transformation of unselective Cu spheres into ethylene-selective Cu cubes. While it still remains an open question, these discrepancies in the literature regarding the behavior of less than 10 nm Cu spheres might also be related to different extent of the surface oxidation of these nanocatalysts. Even if avoided during sample preparation, surface oxidation does occur at open circuit voltage. [39] The impact of the latter on CO$_2$RR might be particularly drastic for these small nanocatalysts where structural effects are absent because of the lack of extended facets.

While the comparison of Cu spheres with single crystal is non-trivial because of their difficult to map number and kind of facets, Cu cubes have provided an ideal platform to gain insight into structural effects in CO$_2$RR. These NCs are enclosed by 6x (100) facets, 12x (110) facets at the

edges and 8x (111) facets at the corners. The first experiments on Cu nanocubes for CO_2RR were conducted by Roberts et al., [28] on a sample with size ~100 nm synthesized via electrochemical cycling. These nanocatalysts exhibited preferential selectivity towards ethylene compared to the polycrystalline copper foil, a finding consistent with the studies on single crystals. In the same year Chen et al. drew the same observation on the selectivity of Cu cuboidal mesocrystals of around 500 nm. [29] However, it was only later, we highlighted the importance of (100)/(110) step-edges for C-C coupling and ethylene production by investigating the catalytic properties of size-controlled Cu cubes synthesized via colloidal chemistry. [1] The selectivity measurements, expressed as faradaic efficiency (FE), revealed that the NCs with edge length around 44 nm possessed the highest FE efficiency (around 40%) for ethylene at -1.1 V_{RHE} (Figure 2A). [1] By the same token, in the past year Zhong et al. [40] highlighted coupling effects at (100)/ (110) sites on Cu foils, and demonstrated that sites at steps between these surfaces are active and selective for C_2+ products. DFT calculations have indeed shown that (110)/(100) steps favour C-C coupling. [41] In turn, this result suggested that the cubes with an average 40 nm size provide an optimal population of the surface sites which maximize ethylene selectivity.

The size-dependent selectivity trends in Cu cubes highlighted the importance to carefully assess size-and-shape dependent relationships also in other catalyst shapes. Indeed, only systematic studies can establish which sites maximize selectivity towards target products. To this end, we investigated the selectivity of the (111) facets towards methane by exploiting size-controlled Cu nanocatalysts with octahedral shape. These NCs are terminated by 8x (111) facets, 12x (110) facets at the edges and 6x (100) corners. The study of the electrocatalytic behavior of Cu octahedra with average sizes of 75 nm, 150 and 310 nm revealed that the smallest possessed the highest faradaic efficiency towards methane, reaching up to 55% at -1.35 V_{RHE} (Figure 2B). [2] These results confirmed that the (111) facets direct selectivity towards methane, consistently with the single crystal study; however, it also revealed again that edge-to-faces ratio plays a crucial role in directing selectivity. Indeed, the nanocatalysts with the largest (110)/(111) ratio displayed the highest CO_2RR and methane selectivity.
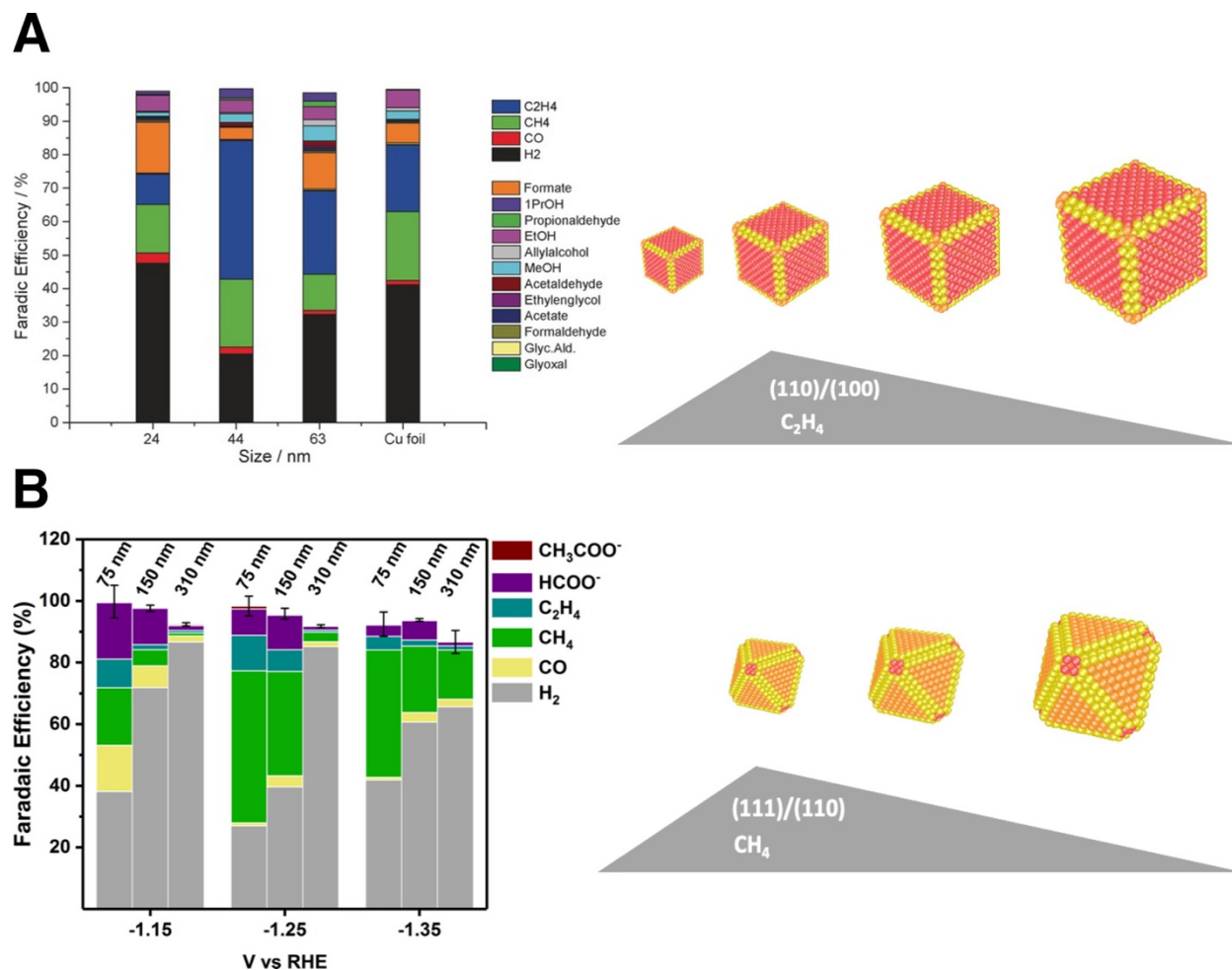
Figure 2. (A) FEs of Cu cubes of three sizes (24, 44 and 60 nm) measured at -1.1V$_{RHE}$ in 0.1M KHCO3 along with a schematic illustration of the main result. Adapted with permission from [1] . Copyright 2016, Wiley. **(B)** Potential-dependent FEs of Cu octahedra of different sizes (75, 150 and 310 nm) measured in 0.1M KHCO3 along with a schematic illustration the main result. Adapted with permission from [2]. Copyright 2019, Royal Society of Chemistry.

Shape-controlled NCs not only enabled to expand on the results drawn from studies on single crystal studies, but also to systematically assess the activity and selectivity of adsorption sites whose number and kind is difficult to isolate in surface science experiments. Active sites at grain boundaries represent a notable example of such sites. While definitive conclusions cannot be made at this stage, a few studies are worth of notice. Feng et al. [42] were among the first to show that the abundance of grain boundaries in polycrystalline Cu spheres correlates with C$_2$ product selectivity.

Choi et al. assessed the interplay between grain boundaries and catalyst faceting on well-defined star decahedron Cu nanocatalysts. [34] While these nanocatalysts exposed mostly (111) surfaces, FEs up to 60% towards ethylene at -1.00 V_{RHE} was found and explained via strain effects arising at the nanoscale. The prominent role of grain boundaries in directing CO$_2$RR selectivity appears also in a study on five-fold twinned nanowires performed by Li et al. [43] Notwithstanding the (100) facets being the most exposed on the surface, FEs up to 55% for methane were measured.

4. SHAPE-CONTROLLED NANOCATALYSTS AND TANDEM SCHEMES TO INTERROGATE CO$_2$RR PATHWAYS

Beyond tuning selectivity by modifying the shape of Cu-only NCs , we have recently illustrated that NCs with well-defined facets and tandem schemes can be combined to interrogate CO$_2$ pathways and tailor the catalyst selectivity beyond the findings from single crystal investigations. To this end, tandem catalysts were prepared by mixing CO-producing Ag spheres with ethylene-producing Cu cubes (Ag-Cu$_{cub}$) and methane-producing Cu octahedra (Ag-Cu$_{oh}$) (Figure 3A) . As illustrated in Figure 3B, the FE towards C$_{2+}$ products increased in both catalysts, consistently with the increased local concentration of CO enhancing C-C coupling. However, Ag-Cu$_{oh}$ were found to selectively improve the FE for ethanol over ethylene and the expenses of methane. The selectivity shift from methane to ethanol in the presence of an increased local concentration of CO suggested that the CO$_2$ to ethanol conversion finds a preferred pathway in CH$_x$-CO coupling on (111) facets while CO-CO coupling still takes place on the (100) facets leading to ethylene formation (Figure 3C). [3] In a recent follow up study, a semi-empirical numerical model has suggested that a greater enhancement of ethanol production is actually expected on the (110)/(100) step sites at the edges of the cubes. However, such effect is mitigated by the larger fraction of (100) facets which continue to produce ethylene. CO$_2$RR experiments on Ag-Cu$_{cub}$ with Cu$_{cub}$ of different sizes corroborated this prediction, by showing that the smaller cubes, which possess the highest (110)/(100) ratio, selectively enhance ethanol production (Figure 3D). [44] This study is a powerful example of the fruitful synergy of theory and size-and-shape controlled nanocatalysts.
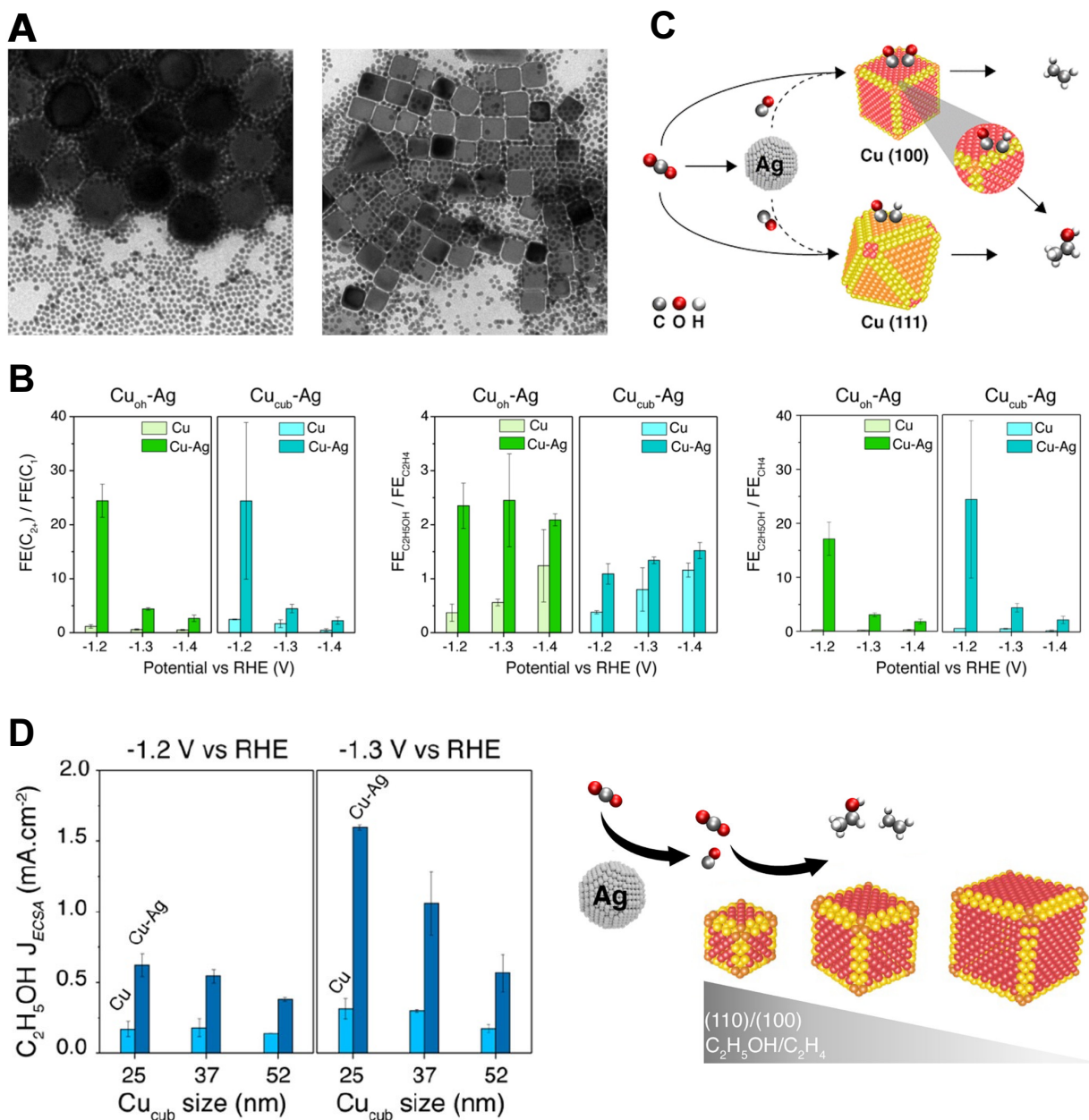
Figure 3. (A) Representative TEM images of the Ag-Cu$_{oh}$ and Ag-Cu$_{cub}$ tandem catalysts. **(B)** FE C$_{2+}$ / FE C$_1$, FE C$_2$H$_5$OH / FE C$_2$H$_4$, and FE C$_2$H$_5$OH /FE CH$_4$ for the the two catalysts in (A) measured at different potentials in 0.1 M KHCO$_3$. **(C)** Schematic representation of the tandem mechanisms on Ag-Cu$_{oh}$ and Ag-Cu$_{cub}$. **(D)** ECSA (Electrochemically active surface area)-normalized current densities for Ag-Cu$_{cub}$ catalysts including different sizes of Cu$_{cub}$ along with a schematic representation of the major finding. Images are adapted with permission from [3] and [44], copyright American Chemical Society.

5. SHAPE-CONTROLLED NANOCATALYSTS TO UNDERSTAND CATALYST RECONSTRUCTION MECHANISMS IN CO₂RR

In addition to enable fundamental insight into structure-selectivity relationships, NCs with precisely defined sizes and shapes are an ideal platform to uncover the mechanisms behind catalyst reconstruction during CO_2RR, which is crucial to eventually being able to control these transformations. Depending on the initial size and shape, catalyst restructuring might occur on very different time-scales and also lead to an improvement or to a degradation of the initially observed catalytic properties. For example, Cu cubes maintain their ethylene selectivity for up to 6 hours but progressively loose it afterwards. [30,32,45,46] Instead, the 7 nm Cu spheres reconstruct already during the start-up phase and, at high loadings, transform into cubes for longer reaction times, which implies increased selectivity for C_{2+} products. [4,47,48] As another example of positive reconstruction, five-fold twinned Cu nanowires, initially exposing (100) terminations, transform into single crystal nanowires exposing high miller index terminations.[49] Upon this change, they are remarkably selective for ethylene, which parallels results previously found on single crystals with a (551) termination, and their activity and selectivity are stable for up 200 hours.

Using the well-defined Cu cubes obtained by means of colloidal chemistry, we have provided some insight into the degradation mechanism of these nanocatalysts.[32] Ex-situ TEM analysis evidenced that a unique nanoclustering mechanism takes place (Figure 4A) and 3D tomography showed that these clusters detached from the edges (Figure 4B), which were indeed identified as the active sites for C-C coupling. Similar degradation pathway starting from the cube edges was also detected by Grosse et al. [30] using operando atomic force microscopy (AFM). Different controlled experiments combined with Grand canonical DFT calculations clarified that the negative potential greatly contributes to such degradation (Figure 4C), thus suggesting that strategies aiming at reducing the overpotential should also contribute to solve the stability issue.

More recently, we monitored the reconstruction of Cu spheres during the start-up phase of CO_2RR by means of electrochemical in situ TEM and operando X-ray absorption spectroscopy (XAS). [4] As illustrated in Figure 4D, the Cu nanocatalysts shrink and then disappear, rather than coalesce. The size monodispersity of the initial sample, combined with the TEM resolution, allowed to

follow the size distribution over time (Figure 4E), which evolve from a narrow size distribution to a bi-modal one at later stages, due to the shrinking of some catalysts, and the growth of others. These results combined with the changes in Cu surface oxidation state observed by operando XAS, suggest that a dissolution/redeposition mechanism which involves Cu transient species dissolved in solution is the route through which the Cu nanocatalyst evolve into bigger sizes (Figure 4F), until eventually transform in cubic particles. [4, 47, 48]
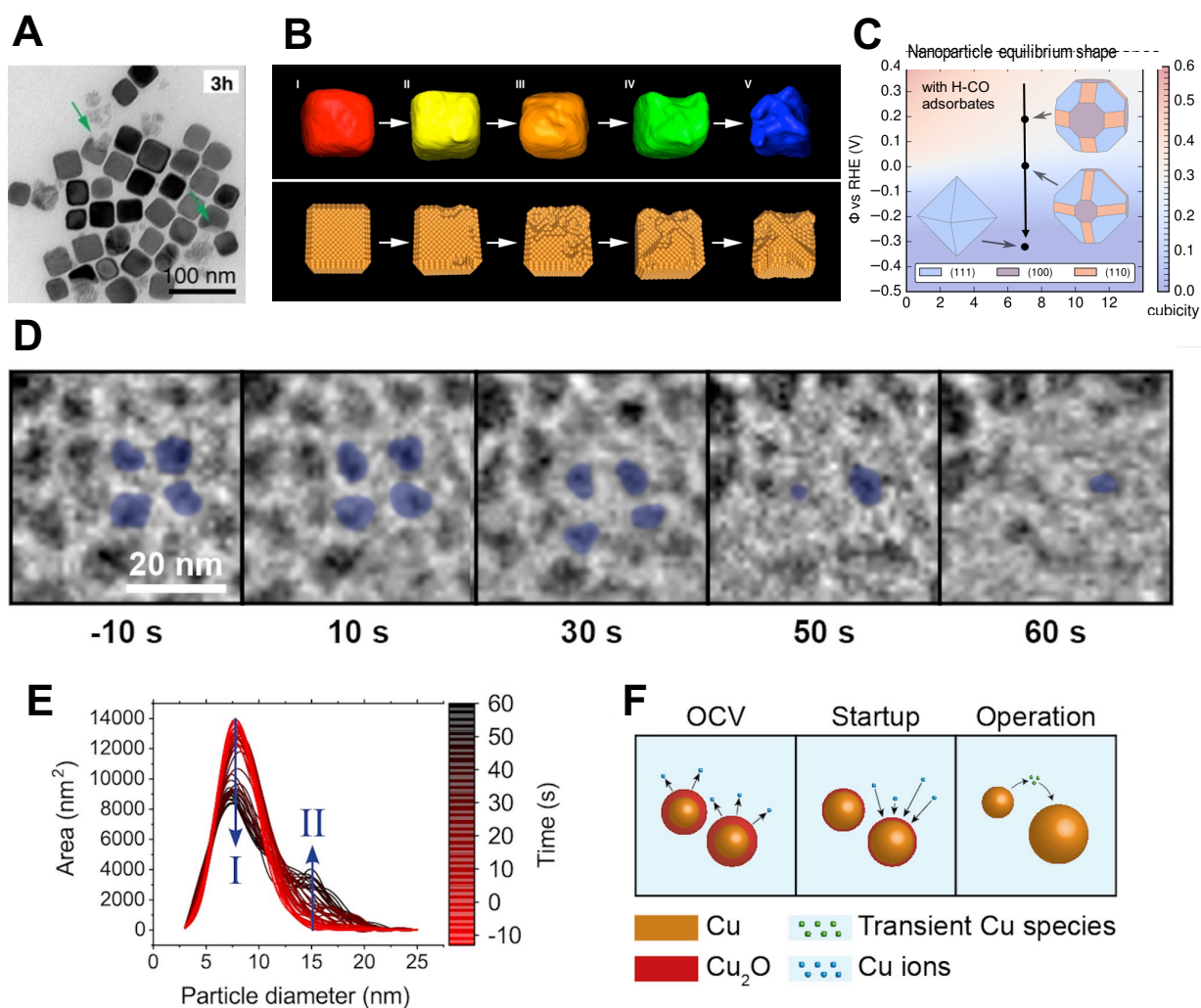

Figure 4. **(A)** TEM image of 44 nm Cu cubes after 3 hours of reaction at -1.1VRHE in 0.1M KHCO₃; the green arrow highlight the formation of small clusters. (B) Tomographic reconstruction of the same and corresponding schematic morphological models at different stages during a 12 h-

course of CO$_2$RR. (C) pH and potential dependence of the Wulff-shape of Cu nanoparticles including H, CO, and mixed H + CO covered surfaces. The cubicity is defined as the relative contribution of Cu (100) surfaces to the Wulff-shape. Taken from [32], Copyright Nature Springer. **(D)** Snapshots of in-situ TEM movie illustrating the shrinking process of 7 nm Cu spheres during the initial stages of CO$_2$RR. **I** Time dependent evolution of the area weighted particle size distribution. Arrow I pinpoints the decrease in the abundance of primary particles, Arrow II highlights the gradual increase in the population of secondary particles **(F)** Schematic representation of the dissolution/deposition mechanism driving the reconstruction of 7 nm Cu spheres. Taken from [4], Copyright Wiley.

6. CONCLUSIONS AND OUTLOOK

The examples showcased in this Account illustrate that tailored NCs with well-defined size and shape are an ideal platform to investigate the structural dependence of CO$_2$RR beyond single crystal studies. At the same time, work has been mostly limited so far to Cu NCs exposing (100), (110) and (111). Instead, both theoretical and experimental single crystal studies suggest interesting selectivity towards oxygenated and multi-carbon products emerging on other surfaces. [50, 51] Therefore, the library of shaped Cu NCs must be enlarged, which represents a motivation to develop further the underexplored chemistry of non-noble metal NCs. [52]

An open debate in the community exists regarding the possibility of translating fundamental studies on shape-controlled Cu NCs to devices under commercially relevant conditions. Recent studies show great promise in this direction and demonstrate positive synergism between catalyst design and device engineering for improving catalyst activity and stability. [45, 46] Yet, more efforts in this direction are needed.

Also related to the application in devices, it is yet to be fully understood how to predict, control, prevent, or exploit, nanocatalyst restructuring under CO$_2$RR conditions. Operando characterization is crucial to unravel the degradation mechanisms. By the same token, theoretical modelling should progress to include a realistic complexity in the simulation of CO$_2$RR nanocatalysts. DFT-based

screening [11,12,53] and molecular dynamics simulations [54,55] allow to draw precious insight about the CO_2 reduction on ideal surfaces, while machine learning potential and high-throughput predictions promise to unlock predictions on more realistic representation of the catalysts. [56,57,58] In the future we expect increasing synergies between experiment and theory to unravel the activity and selectivity of nanostructured surface sites, and understanding more in depth the dynamic restructuring of nanocatalysts under operation.

AUTHOR INFORMATION

Corresponding Author

Raffaella Buonsanti − Laboratory of Nanochemistry for Energy (LNCE), Department of Chemical Sciences and Engineering, École Polytechnique Fédérale de Lausanne, CH-1950 Sion, Switzerland; orcid.org/0000-0002-6592-1869;
Email: raffaella.buonsanti@epfl.ch

Other Authors

Kevin Rossi − Laboratory of Nanochemistry for Energy (LNCE), Department of Chemical Sciences and Engineering, École Polytechnique Fédérale de Lausanne, CH-1950 Sion, Switzerland

Complete contact information is available at:
https://pubs.acs.org/10.1021/acs.accounts.0c00698

Biographies

Raffaella Buonsanti received her master degree in Chemistry from the University of Bari. After been awarded her PhD in Nanochemistry from the University of Salento working at the National Nanotechnology Laboratory, she spent almost six years at Lawrence Berkeley National Laboratory, first as a postdoctoral researcher and project scientist at the Molecular Foundry, later

as a staff scientist at the Joint Center of Artificial Photosynthesis. Since 2015, she is a tenure-track Assistant Professor in the Institute of Chemical Sciences and Engineering at the École Polytechnique Fédérale de Lausanne. She leads a broad multidisciplinary program which spans from materials chemistry and nanoscience to catalysis, electrochemistry and sustainability. Her team is interested in the synthetic development of nanocrystals and their use as electrocatalysts to drive the conversion of small molecule and as materials to advance different energy technologies.

Kevin Rossi obtained his PhD in Physics from King's College London in 2019 under the supervision of Prof. Baletto. He then undertook a Postdoc researcher role in Prof. Ceriotti's lab at the Ecole Polytechnique Fédérale de Lausanne (Switzerland) between 2018 and 2020. Since September 2020 he has been a Marie Curie Sklodowska Fellow hosted in Prof. Buonsanti's lab. His research focuses on the use of numerical and data-driven methods to address problems of relevance to green energy and green chemistry.

REFERENCES
(1) Loiudice, A.; Lobaccaro, P.; Kamali, E. A.; Thao, T.; Huang, B. H.; Ager, J.; Buonsanti, R. Tailoring copper nanocrystals towards C_2 products in electrochemical CO_2 reduction. Angew. Chem. Int. Ed. **2016**, 55 (19), 5789-5792

(2) Iyengar, P.; Huang, J.; De Gregorio, G.L.; Gadiyar, C.; Buonsanti, R. Size dependent selectivity of Cu nano-octahedra catalysts for the electrochemical reduction of CO_2 to CH_4. Chem. Comm. **2020**, 55 (60), 8796-8799

(3) Iyengar, P.; Kolb, M. J.; Pankhurst, J. R.; Calle-Vallejo, F.; Buonsanti, R. Elucidating the Facet-Dependent Selectivity for CO_2 Electroreduction to Ethanol of Cu–Ag Tandem Catalysts. ACS Catal. **2021**, 11 (8), 4456-4463

(4) Vavra, J.; Shen, T.; Stoian, D.; Tileli, V.; Buonsanti, R. Real-time Monitoring Reveals Dissolution/Redeposition Mechanism in Copper Nanocatalysts during the Initial Stages of the CO_2 Reduction Reaction. Angew. Chem. Int. Ed. **2021**, 60 (3),1347-1354.

(5) Nitopi, S; Bertheussen, E.; Scott, S. B.; Liu, X.; Engstfeld, A. K.; Horch, S.; Seger, B.; Stephens, I. E. L.; Chan, K.; Hahn, C.; Nørskov, J. K.; Jaramillo, T. F.; Chorkendorff I. Progress and Perspectives of Electrochemical CO_2 Reduction on Copper in Aqueous Electrolyte. Chem. Rev. **2019** 119 (12), 7610-7672

(6) De Luna, P.; Hahn, C.; Higgins, D.; Jaffer, S.A.; Jaramillo, T.F.; Sargent, E. H. What would it take for renewably powered electrosynthesis to displace petrochemical processes? Science **2019** 26;364(6438):eaav3506.

(7) Haas, T.; Krause, R.; Weber, R.; Demler, M.; Schmid, G. Technical photosynthesis involving CO2 electrolysis and fermentation. Nat. Catal. **2018**, 1, 32–39

(8) Pace, G.; Sheehan, S. W. Scaling CO_2 Capture With Downstream Flow CO2 Conversion to Ethanol. Front. in Clim. **2021**, 3, 656108

(9) Kuhl, K. P.; Cave, E. R.; Leonard., G. Reactor with advanced architecture for the electrochemical reaction of CO_2, CO, and other chemical compounds. U.S. Patent Number 10648091 May 12, **2020**

(10) Hori, Y. Electrochemical CO_2 Reduction on Metal Electrodes. In Modern Aspects of Electrochemistry, Vayenas, C. G.; White, R. E.; Gamboa-Aldeco, M. E., Eds.; Springer, **2008**; 42, 89−189.

(11) Bagger, A.; Ju, W.; Varela, A. S.; Strasser, P.; Rossmeisl, J. Electrochemical CO_2 Reduction: A Classification Problem. Chem. Phys. Chem. **2017**, 18, 3266−3273.

(12) Liu, X.; Xiao, J.; Peng, H.; Hong, X.; Chan, K.; Nørskov, J. K. Understanding trends in electrochemical carbon dioxide reduction rates. Nat. Comm. **2017**, 8 15438.

(13) Kuhl, K. P.; Cave, E. R.; Abram, D. N.; Jaramillo, T. F. New Insights into the Electrochemical Reduction of Carbon Dioxide on Metallic Copper Surfaces. Energy Environ. Sci. **2012**, 5, 7050−7059.

(14) Hori, Y.; Takahashi, I.; Koga, O.; Hoshi, N. Electrochemical Reduction of Carbon Dioxide at Various Series of Copper Single Crystal Electrodes. J. Mol. Catal. A: Chem. **2003**, 199, 39−47.

(15) Hahn, C.; Hatsukade, T.; Kim, Y. G.; Vailionis, A.; Baricuatro, J. H.; Higgins, D. C.; Nitopi, S. A.; Soriaga, M. P.; Jaramillo, T. F. Engineering Cu Surfaces for the Electrocatalytic Conversion

of CO$_2$: Controlling Selectivity toward Oxygenates and Hydrocarbons. Proc. Natl. Acad. Sci. **2017**, 114, 5918−5923

(16) Huang, Y.; Handoko, A. D.; Hirunsit, P.; Yeo, B. S. Electrochemical Reduction of CO$_2$ Using Copper Single-Crystal Surfaces: Effects of CO* Coverage on the Selective Formation of Ethylene. ACS Catal. **2017**, 7, 1749−1756

17) Schouten, K. J. P.; Pérez Gallent, E.; Koper, M. T. M. Structure Sensitivity of the Electrochemical Reduction of Carbon Monoxide on Copper Single Crystals ACS Catal. **2013**, 3, 6, 1292–1295.

(18) Editorial. Mind the gap. Nat. Catal. **2018**, 1, 807–808

(19) Sheehan, S.W.; Buonsanti, R. Deriving value from CO$_2$: from catalyst design to industrial implementation. Chem Catalysis. **2021**, 1, 4, 751-753

(20) Chen, J. G.; Jones, C. W.; Linic, S.; Stamenkovic, V. R. Best Practices in Pursuit of Topics in Heterogeneous Electrocatalysis. ACS Catal. **2017**, 7, 9, 6392- 6393

(21) Chatenet, M.; Benzigerb, J.; Inabac, M.; Kjelstrupd, S.; Zawodzinskie, T.; Raccichini, R. Good practice guide for papers on fuel cells and electrolysis cells for the Journal of Power Sources. J Pow. Sour. **2020**, 451, 227635

(22) Lin, H.; Wei, K.; Yin, Z.; Sun, S.; Nanocatalysts in electrosynthesis, Iscience, **2021**, 24, 3, 102172

(23) Guntern, Y. T.; Okatenko, V.; Pankhurst, J.; Varandili, S. B.; Iyengar, P.; Koolen, C.; Stoian, D.; Vavra, J.; Buonsanti, R.. Colloidal Nanocrystals as Electrocatalysts with Tunable Activity and Selectivity. ACS Catal. **2021**, 11, 3, 1248-1295

(24) Cargnello, M.; Colloidal Nanocrystals as Building Blocks for Well-Defined Heterogeneous Catalysts Chem. Mater. **2019**, 31, 576−596

(25) Xia, Y.; Xiong, Y.; Lim, B.; Skrabalak, S.E. Shape-controlled synthesis of metal nanocrystals: simple chemistry meets complex physics? Angew. Chem. Int. ed., 2008, 48, 1, 60-103

(26) Huang, J.; Buonsanti, R. Colloidal Nanocrystals as Heterogeneous Catalysts for Electrochemical CO$_2$ conversion. Chem. Mat., 2018, 31 (1) 13-25

(27) Reske, R.; Mistry, H.; Behafarid, F.; Roldan Cuenya, B.; Strasser, P. Particle Size Effects in the Catalytic Electroreduction of CO$_2$ on Cu Nanoparticles. J. Am. Chem. Soc. **2014**, 136, 19, 6978–6986

(28) Roberts, F. S.; Kuhl, K. P.; Nilsson, A. High Selectivity for Ethylene from Carbon Dioxide Reduction over Copper Nanocube Electrocatalysts. Angew. Chem. Int. Ed. **2015**, 127, 17, 5268-5271.

(29) Chen, C. S.; Handoko, A. D.; Wan, J. H.; Ma, L.; Rena, D.; Yeo, B.S. Stable and selective electrochemical reduction of carbon dioxide to ethylene on copper mesocrystals. Catal. Sci. Technol., **2015**, 5, 161-168

(30) Grosse, P.; Gao, D.; Scholten, F.; Sinev, I.; Mistry, H.; Roldan Cuenya, B. Dynamic Changes in the Structure, Chemical State and Catalytic Selectivity of Cu Nanocubes during CO_2 Electroreduction: Size and Support Effects. Angew Chem. Int. ed. **2018**, 51, 21, 6192-6297

(31) Manthiram, K.; Beberwyck, J.; Alivisatos, A. P. Enhanced electrochemical methanation of carbon dioxide with a dispersible nanoscale copper catalyst. J. Am. Chem. Soc. **2014**, 136, 38, 13319-25

(32) Huang, J.; Hormann, N.; Oveisi, E.; Loiudice, A.; De Gregorio, G.L.; Andreussi, O.; Marzari , N.; Buonsanti, R. Potential-induced nanoclustering of metallic catalysts during electrochemical CO_2 reduction. Nat. Comm. **2018**, 9 (1), 1-9

(33) Strach, M.; Mantella, V.; Pankhurst, J. R.; Iyengar, P.; Loiudice, A.; Das, S.; Corminboeuf, C.; van Beek, W.; Buonsanti, R. Insights into Reaction Intermediates to Predict Synthetic Pathways for Shape-Controlled Metal Nanocrystals. J. Am. Chem. Soc. **2019**, 141, 41, 16312–16322

(34) Choi, C.; Cheng, T.; Flores Espinosa, M.; Fei, H.; Duan, X.; Goddard III, W. A.; Huang, Y. A Highly Active Star Decahedron Cu Nanocatalyst for Hydrocarbon Production at Low Overpotentials. Adv. Mat. **2019**, 31, 6, 1805405.

(35) Wang, Z.; Yang, G.; Zhang, Z.; Jin, M.; Yin, Y. Selectivity on Etching: Creation of High-Energy Facets on Copper Nanocrystals for CO_2 Electrochemical Reduction. ACS Nano **2016**, 10, 4, 4559–4564

(36) Xia, Y.; Xia, X.; Peng, H. Shape-Controlled Synthesis of Colloidal Metal Nanocrystals: Thermodynamic versus Kinetic Products. J. Am. Chem. Soc. **2015**, 137, 7947−7966

(37) Mistry, H.; Behafarid, F.; Reske, R.; Varela, A. S.; Strasser, P.; Roldan Cuenya, B. Tuning Catalytic Selectivity at the Mesoscale via Interparticle Interactions. ACS Catal. **2016**, 6, 2, 1075–1080

(38) Kim, D.; Kley, C.S.; Li, Y.; Yang, P. Copper nanoparticle ensembles for selective electroreduction of CO_2 to C_2-C_3 products. Proc. Natl. Acad. Sci. **2017**, 114 (40), 10560-10565

(39) Hochfilzer, D.; Sørensen, J.E.; Clark, E.L.; Scott, S.B.; Chorkendorff, I.; Kibsgaard, J. ACS Ener. Lett. 2021, 6, 5, 1879-1885

(40) Zhong, J.; Zhao, Z.; Zhao, Q.; Cheng, D.; Liu, B.; Zhang, G.; Deng, W.; Dong, H.; Zhang, L.; Li, J.; Li, J.; Gong J. Coupling of Cu(100) and (110) Facets Promotes Carbon Dioxide Conversion to Hydrocarbons and Alcohols. Angew.Chem. Int. Ed. **2021**, 60,4879–4885

(41) Mangione, G.; Huang, J.; Buonsanti, R.; Corminboeuf, C. Dual-Facet Mechanism in Copper Nanocubes for Electrochemical CO_2 Reduction into Ethylene. J. Phys. Chem. Lett. **2019**, 10, 15, 4259–4265.

(42) Feng, X.; Jiang, K.; Fan, S.; Kanan, M. W. A Direct Grain-Boundary-Activity Correlation for CO Electroreduction on Cu Nanoparticles. ACS Cent. Sci. **2016**, 2, 3, 169–174.

(43) Li, Y.; Cui, F.; Ross, M. B.; Kim, D.; Sun, Y.; Yang, P.; Structure-Sensitive CO_2 Electroreduction to Hydrocarbons on Ultrathin 5-fold Twinned Copper Nanowires. Nano Lett. **2017**, 17, 2, 1312–1317.

(44) Iyengar, P.; Kolb, M.; Pankhurst, J. R.; Calle-Vallejo, F.; Buonsanti, R. Theory-guided enhancement of CO_2 reduction to ethanol on Ag-Cu tandem catalysts via particle-size effects. ACS Catal. **2021**, 11, 13330-13336

(45) De Gregorio, G. L.; Burdyny, T.; Loiudice, A.; Iyengar, P.; Smith, W. A.; Buonsanti, R. Facet-Dependent Selectivity of Cu Catalysts in Electrochemical CO_2 Reduction at Commercially Viable Current Densities ACS Catal. **2020**, 10, 9, 4854–4862

(46) Wang, Y.; Shen, H.; Livi, K. J. T.; Raciti, D.; Zong, H.; Gregg, J.; Onadeko, M.; Wan, Y.; Watson, A.; Wang, C. Copper Nanocubes for CO_2 Reduction in Gas Diffusion Electrodes. Nano Lett. **2019**, 19, 12, 8461–8468

(47) Osowiecki, W. T.; Nussbaum, J. J.; Kamat, G. A.; Katsoukis, G.; Ledendecker, M.; Frei, H.; Bell, A. T.; Alivisatos, A. P. Factors and Dynamics of Cu Nanocrystal Reconstruction under CO_2 Reduction. ACS Appl. Energy Mater. **2019**, 2, 11, 7744–7749.

(48) Kuang, S.; Li, M.; Xia, R.; Xing, L.; Su, Y.; Fan, Q.; Liu, J.; Hensen, E. J. M.; Ma, X.; Zhang S. Stable Surface-Anchored Cu Nanocubes for CO_2 Electroreduction to Ethylene. ACS Appl. Nano Mater. **2020**, 3, 8, 8328–8334.

(49) Choi, C.; Kwon, S.; Cheng, T.; Xu M.; Tieu P.; Lee C.; Cai J.; Pan X.; Duan X.; Goddard III W.; Huang, Y. Highly active and stable stepped Cu surface for enhanced electrochemical CO_2 reduction to C_2H_4. Nat. Catal, **2020**, 3, 804–812.

(50) Hahn, C.; Hatsukade, T.; Kim, Y.; Vailionis, A.; Baricuatro, J.H.; Higgins, D.C.; Nitopi, S.A.; Soriaga, M.P.; Jaramillo, T.F. Selectively converting CO_2 to chemicals on copper. Proc. Natl. Acad. Sci. **2017**, 114 (23) 5918-5923

(51) Bagger, A.; Ju, W.; Varela, A.S.; Strasser, P.; Rossmeisl, J. Electrochemical CO_2 Reduction: Classifying Cu Facets. ACS Catal. **2019**, 9, 9, 7894-7899

(52) Mantella, V.; Castilla-Amoros, L.; Buonsanti R. Shaping non-noble metal nanocrystals via colloidal chemistry, Chem. Sci. **2020**, 11, 42, 11394-11403

(53) Hussain, J.; Jónsson, H.; Skúlason, E. Calculations of Product Selectivity in Electrochemical CO_2 Reduction. ACS Catal. **2018**, 8, 6, 5240–5249.

(54) Cheng, T.; Fortunelli, A.; Goddard III, W. A. Reaction intermediates during operando electrocatalysis identified from full solvent quantum mechanics molecular dynamics. Proc. Natl. Acad. Sci. **2019** 116 (16) 7718-7722.

(55) Yang, H.; Negreiros, F. R.; Sun, Q.; Xie, M.; Sementa, L.; Stener, M.; Ye, Y.; Fortunelli, A.; Goddard III, W. A., Cheng T. Predictions of Chemical Shifts for Reactive Intermediates in CO_2Reduction under Operando Conditions. ACS Appl. Mater. Interfaces **2021**, 13, 27, 31554–31560.

(56) Gazzarrini, E.; Rossi, K.; Baletto, F.; Born to be different: the formation process of Cu nanoparticles tunes the size trend of the activity for CO_2 to CH_4 conversion. Nanosc. **2021**,13, 5857-5867.

(57) Cheng, D.; Zhao, Z.; Zhang, G.; Yang, P.; Li, L.; Gao, H.; Liu, S.; Chang, X.; Chen, S.; Wang, T.; Ozin, G. A.; Liu, Z.; Gong, J. The nature of active sites for carbon dioxide electroreduction over oxide-derived copper catalysts. Nat. Comm. **2021** 12, 395.

(58) Huang, Y.; Chen, Y.; Cheng, T.; Wang, L.; Goddard III, W. A. Identification of the Selective Sites for Electrochemical Reduction of CO to C_{2+} Products on Copper Nanoparticles by Combining Reactive Force Fields, Density Functional Theory, and Machine Learning. ACS Ener. Lett. **2018**, 3, 12, 2983–2988.

Size-Controlled Nanocrystals

Shape-Controlled Nanocrystals

Selective Cu nanocatalysts for CO₂RR

Data-Driven & Numerical Methods

Single Crystal Experiments

Materials Chemistry